Supplementary Materials for

Antigen-specific memory NK cell responses against HIV and influenza utilize the NKG2/HLA-E axis

Stephanie Jost *et al*.

Corresponding author: R. Keith Reeves, keith.reeves@duke.edu

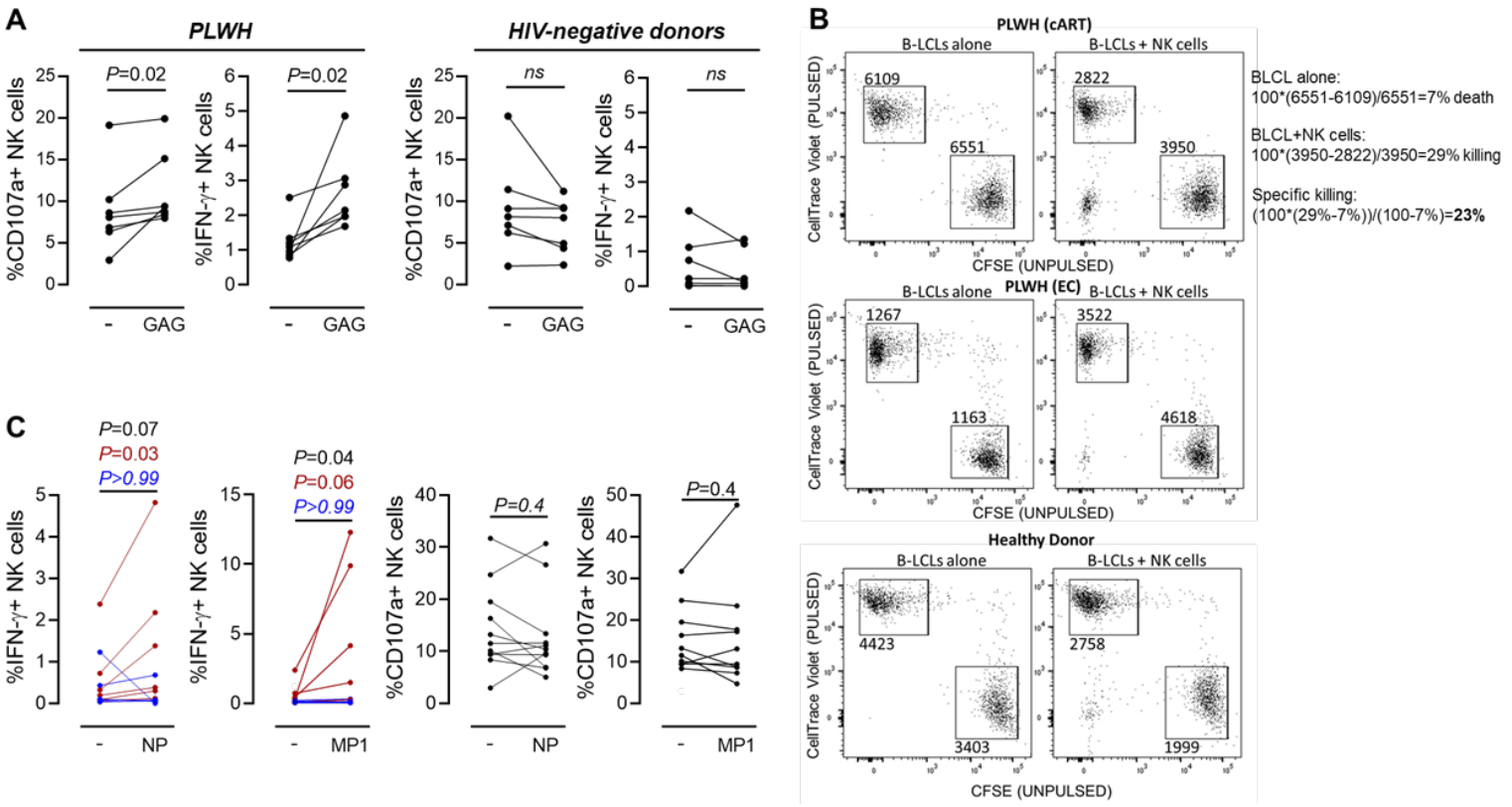

Supplementary Fig. 1. Human primary NK cells mediate antigen-specific responses against HIV and influenza. (A) Enriched NK cells from 7 PLWH (left panels) and 7 HIV-negative healthy donors (right panels) were co-cultured with autologous BLCL that had been pulsed with 2ug/mL peptide pools derived from HIV Gag (HIV-1 Consensus B; provided by the NIH AIDS Reagent Program) and NK cell responses assessed by ICS. Dead cells were excluded. Paired plots show proportions of CD107a+ and IFN-γ+ NK cells in the absence (unstimulated) or presence of the peptide pool. Statistical significance was tested using Wilcoxon signed-rank test. ns, not significant. **(B)** Representative flow cytometry plots depicting CellTrace Violet-stained HIV Gag peptide-pulsed and CFSE-stained unpulsed BLCL from a cART-treated PLWH (upper panels), an elite controller (EC) (middle panels) and a healthy donor (lower panels) alone (left panels) or in the presence of autologous purified NK cells (right panels), after gating on CD3neg CD19pos lymphocytes. Representative example of specific lysis calculation is provided based on the following formula: (% sample lysis with NK effectors - % basal lysis without NK effectors) / (100 - % basal lysis without NK effectors). **(C)** Enriched NK cells from 11 HIV-negative healthy donors were incubated overnight with 2ug/mL peptide pools derived from influenza A/California/04/2009(H1N1) NP and A/California/08/2009(H1N1) MP1 and NK cell responses assessed by ICS. Dead cells were excluded. Paired plots show proportions of IFN-γ^+ and CD107a$^+$ NK cells in the absence (unstimulated) or presence of indicated peptide pools. For IFN-γ, p-values are indicated for all donors (in black) and for donors displaying responses at least 2-fold above (in red) or less than 2-fold above (in blue) unstimulated. Statistical significance was tested using Wilcoxon signed-rank test (**A** and **C**).

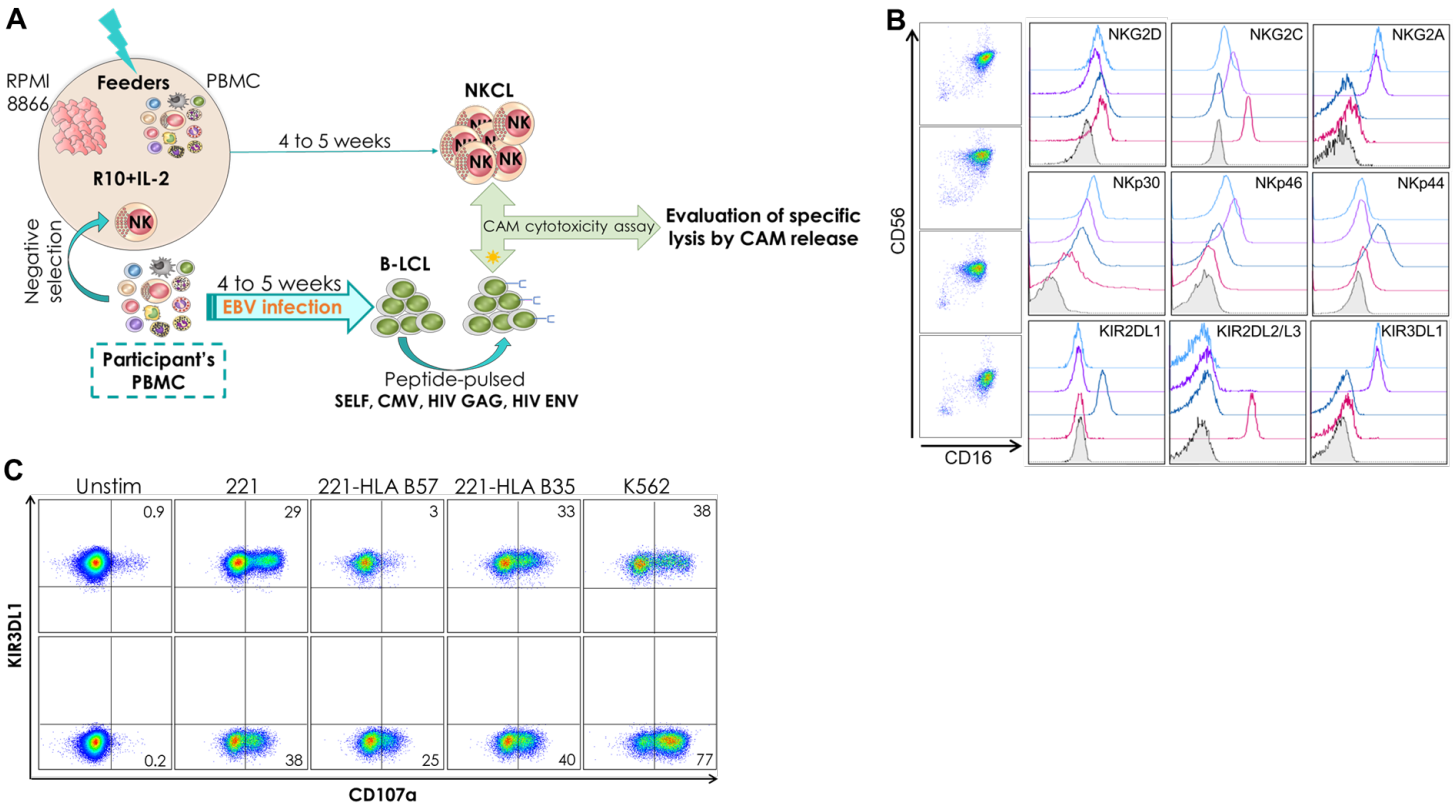

Supplementary Fig. 2. Generation and characterization of human NK cell clones (NKCL). **(A)** Graphical design of the methodology to generate NKCL and evaluate their cytotoxic potential against autologous BLCL presenting viral antigens. (**B)** Representative flow cytometry plots showing CD16 and CD56 expression as well as differential expression of 9 typical NK cell markers on four different NKCL generated from PBMC of one single individual. Colored histograms represent the fluorescence intensity of indicated surface markers expression on NK cells. Tinted grey histograms show the background fluorescence of each investigated antibody determined using an FMO (Fluorescence Minus One) control. **(C)** Functional analysis of peripheral blood NKCL. CD107a upregulation was measured by flow cytometry after incubation of NK cell clones with indicated target cells at a 1:1 E:T ratio. As expected, activation of an exemplary KIR3DL1-expressing NK cell clone was inhibited by the expression of the cognate HLA-Bw4 ligand (here HLA-B57) on 221 cells, but not by HLA-Bw6 molecules (here HLA-B35). NKCL responded to 221 cells, 221 cells expressing HLA-B35 and K562 cells independently of KIR3DL1 expression.

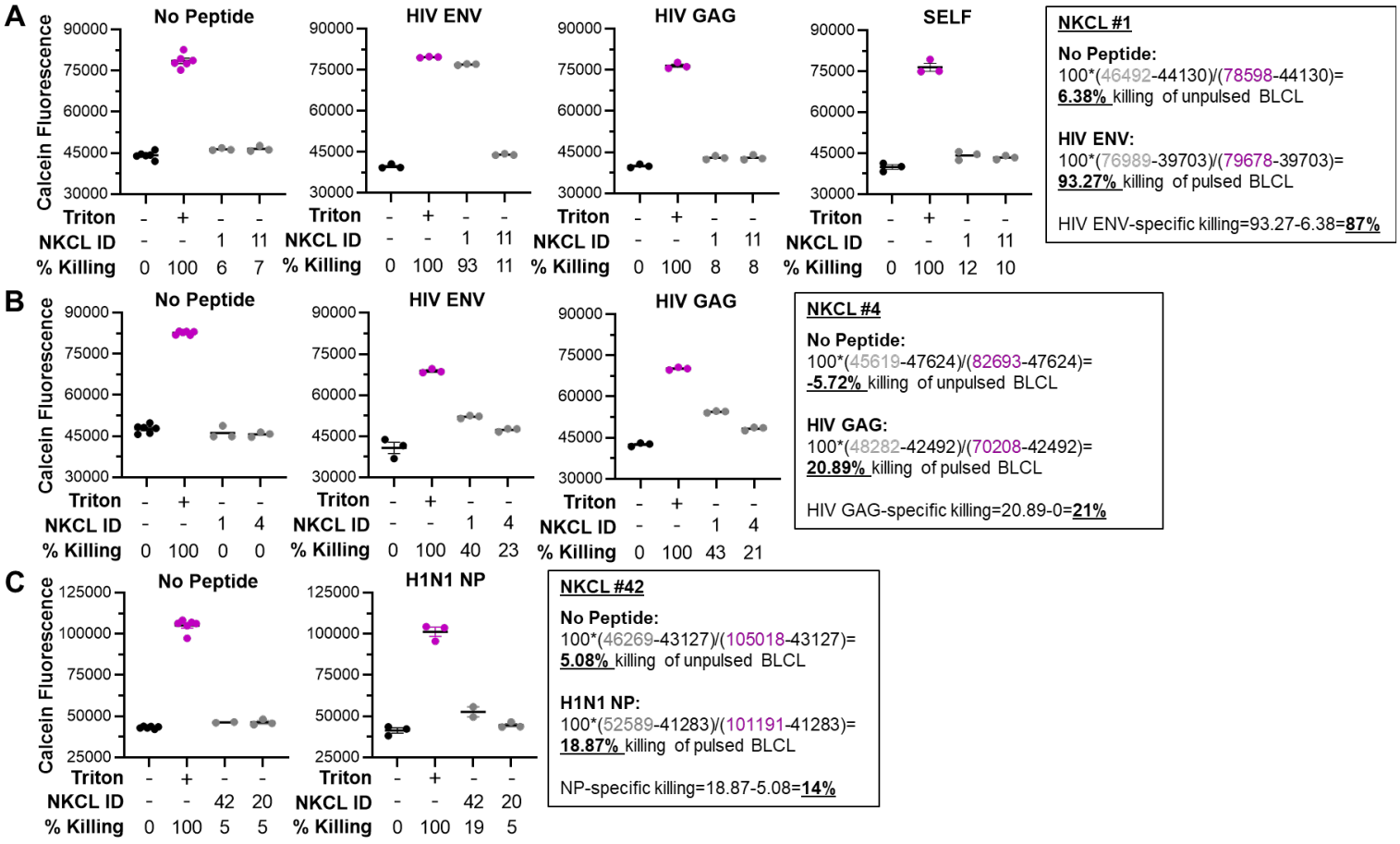

Supplementary Fig. 3. Measures of antigen-specific responses by NKCL using CAM cytotoxicity assays. Representative plots displaying unmodified calcein fluorescence data reflecting release of CAM into the supernatant upon target cell lysis and measured using a Perkin Elmer fluorescence reader (excitation 485 nm, absorption 530 nm) **(A)** for 2 NKCL, including one with (NKCL 1) and one without (NKCL 11) HIV Env-specific killing activity, from one PLWH, **(B)** for 2 NKCL responding to both HIV Env and HIV Gag (NKCL 1 and 4) from another PLWH and **(C)** for 2 NKCL, including one with (NKCL 42) and one without (NKCL 20) influenza H1N1 NP-specific killing activity, from one healthy donor. Examples of percent-specific lysis calculation for two NKCL are provided: (test release – spontaneous release)/(maximum release - spontaneous release) x 100, where spontaneous release is obtained from wells containing target cells in the absence of effector cells or triton (black dots), maximum release from wells containing target cells in the absence of effector cells and addition of triton (purple dots) and test release from wells containing effector and target cells at a 5:1 E:T ratio (grey dots).

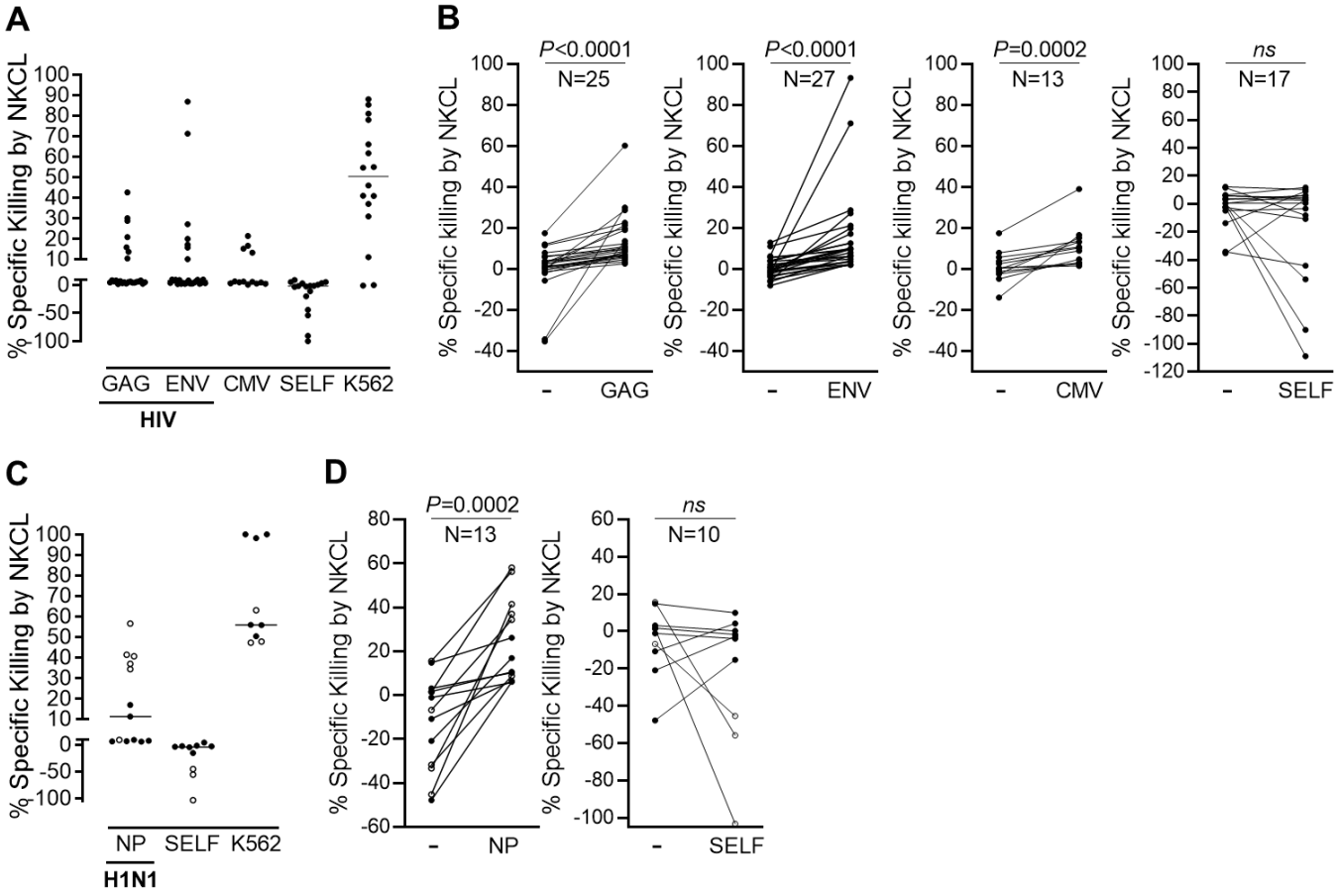

Supplementary Fig. 4. Single-cell cloning of human antigen-specific NK cells. Percentages of antigen-specific lysis by 50 NKCL generated from 12 PLWH against HIV Gag-, HIV Env-, CMV pp65-, and self-antigen-derived peptide pools or HLA-deficient K562 cells **(A),** after subtracting background (mock-pulsed BLCL) and **(B),** compared to non-specific killing of mock-pulsed BLCL for each NKCL. Percentages of antigen-specific lysis by 13 NKCL generated from 4 healthy donors against influenza H1N1 NP- and self-antigen-derived peptide pools or HLA-deficient K562 cells **(C)**, after subtracting background (mock-pulsed BLCL) and **(D)**, compared to non-specific killing of mock-pulsed BLCL for each NKCL. Full circle, positive for IgG antibodies against influenza A. Empty circle, not tested for the presence of IgG antibodies against influenza A. CAM cytotoxicity assays were used to evaluate lysis after co-culture of NKCL with autologous BLCL pulsed with indicated peptide pools. Non-specific lysis was assessed by measuring killing of mock-pulsed autologous BLCL, self-peptides-pulsed BLCL (negative control) and HLA-deficient K562 cells (positive control). Statistical significance was tested using Wilcoxon signed-rank test (**B** and **D**). ns, not significant.

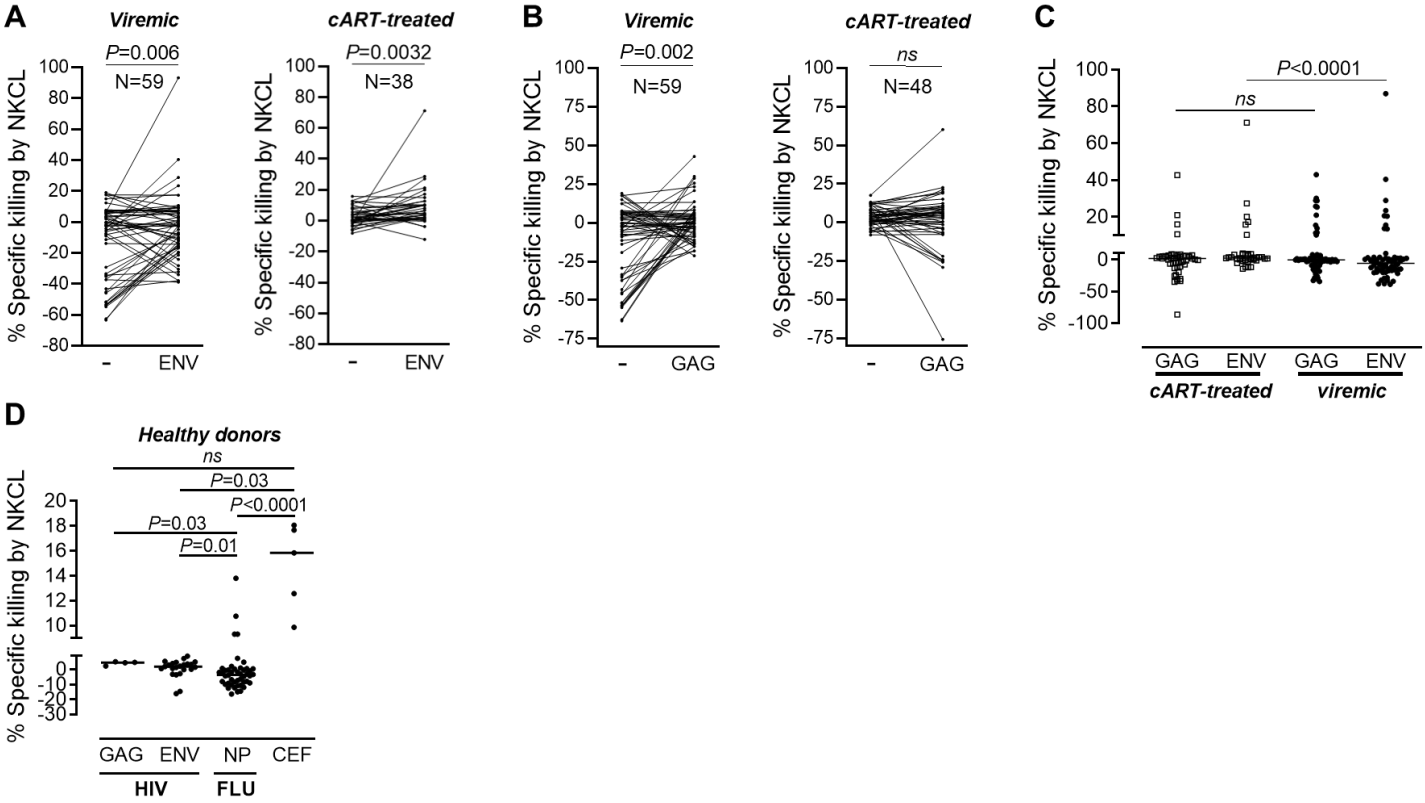

Supplementary Fig. 5. HIV-specific responses by NKCL generated from cART-treated PLWH, untreated viremic PLWH and HIV naïve healthy donors. (A)(B) Paired plots displaying percentages of antigen-specific lysis by 133 NKCL generated from 4 cART-treated PLWH and 16 untreated viremic PLWH against HIV Env **(A)** or HIV Gag **(B)** compared to non-specific killing of mock-pulsed BLCL for each NKCL and **(C)** after subtracting background (mock-pulsed BLCL). **(D)** Percentages of antigen-specific lysis by 63 NKCL generated from 11 HIV-negative healthy donors against HIV Gag-, HIV Env-, influenza H1N1 NP-derived peptides and a pool of CMV, EBV and influenza peptides after subtracting background (mock-pulsed BLCL). CAM cytotoxicity assays were used to evaluate lysis after co-culture of NKCL with autologous BLCL pulsed with indicated peptide pools. Statistical significance was tested using Wilcoxon signed-rank tests (a and b), Mann-Whitney U tests **(A)**, or Kruskal Wallis tests with Dunn's multiple comparison test **(D)**. ns, not significant.

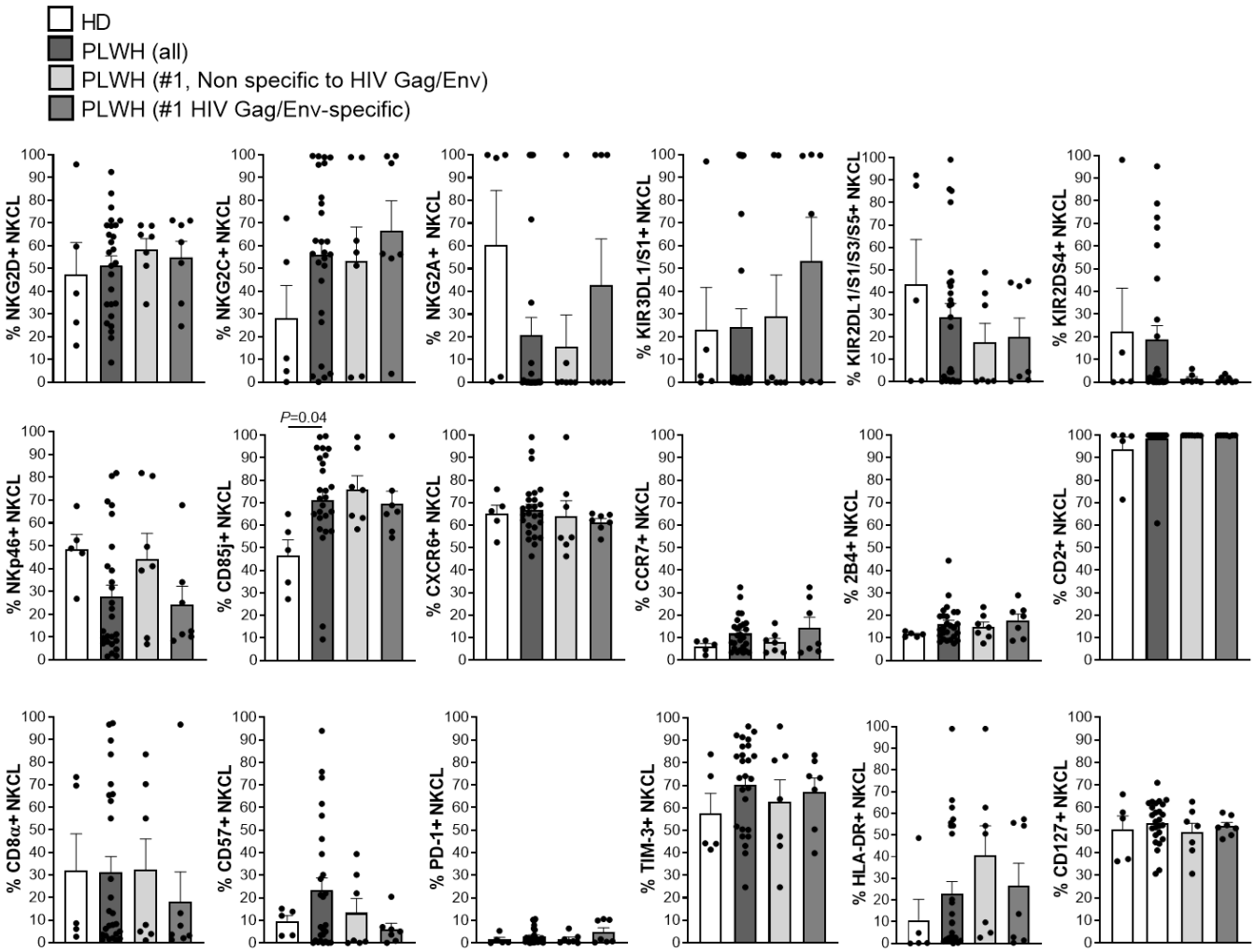

Supplementary Fig. 6. Phenotypic analysis of NKCL generated from PLWH and HIV naïve healthy donors. Bar graphs show mean + SEM proportions of NKCL expressing indicated surface markers evaluated by flow cytometry and comparing 5 NKCL from 2 healthy donors (HD, white bars) with 14 NKCL from one untreated viremic PLWH (darker grey bars), including 7 HIV Gag/Env-specific NKCL (dark grey bars) and 7 NKCL that did not react to HIV Gag/Env (light grey bars).

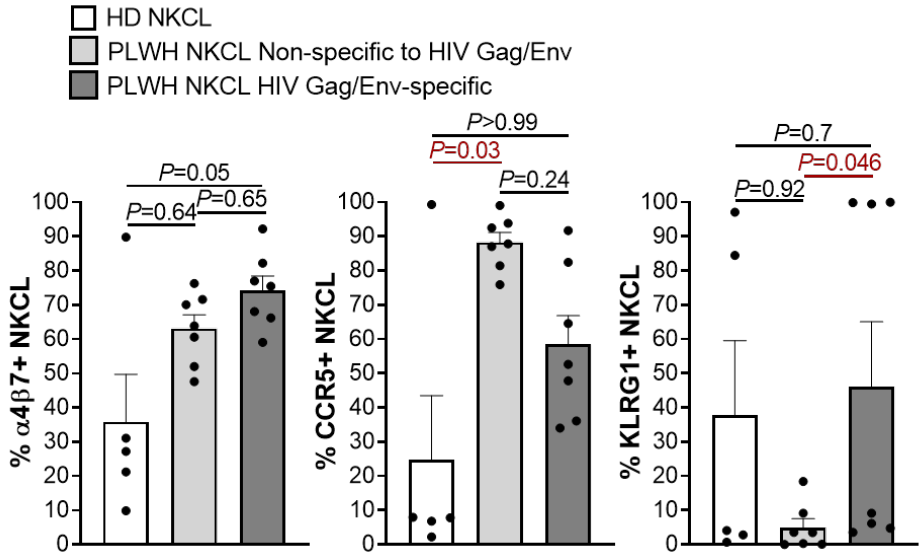

Supplementary Fig. 7. Phenotypic differences between HIV reactive and non-HIV reactive NKCL. Bar graphs show mean + SEM proportions of NKCL expressing α4β7, CCR5 and KLRG1 evaluated by flow cytometry and comparing 5 NKCL from 2 healthy donors (HD) with 14 NKCL from one untreated viremic PLWH, including 7 HIV Gag/Env-specific NKCL and 7 NKCL that did not react to HIV Gag/Env. Statistical significance was tested using Kruskal Wallis test with Dunn's multiple comparison test. Statistically significant p-values are indicated in red.

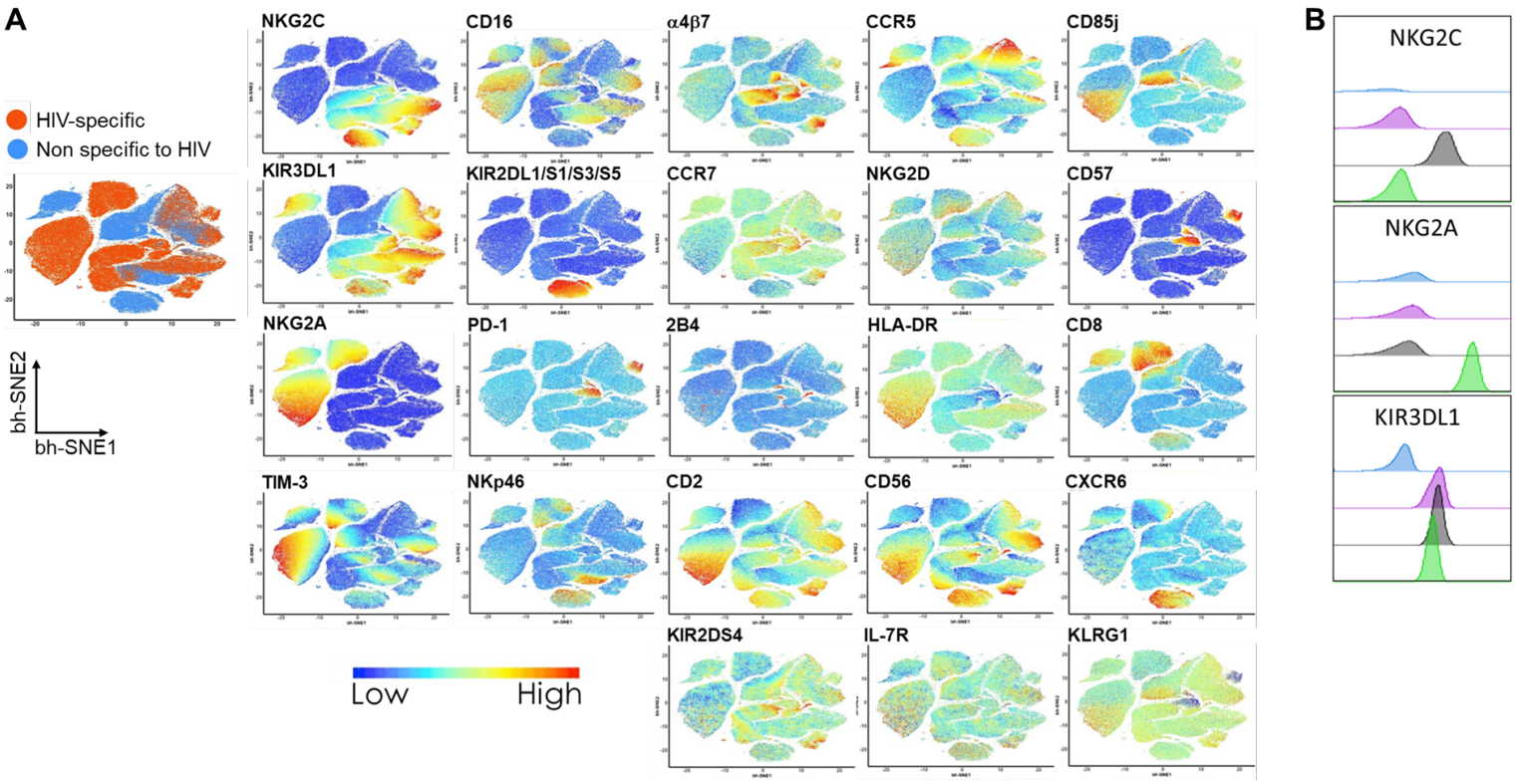

Supplementary Fig. 8. HIV reactive NKCL are associated with NKG2A or NKG2C and/or KIR3DL1 expression. (A) Multidimensional data analysis of 14 NKCL from one untreated viremic PLWH. Live NKCL were analyzed by *t*-SNE with bh-SNE to generate plots clustering cells with similar expression profiles. Relative expression of indicated NK cell markers visualized over the bh-SNE plots is displayed as a colorimetric scale of blue (low expression) to red (high expression). **(B)** Representative flow cytometry histograms displaying differential expression profiles of NKG2C, NKG2A and KIR3DL1 on 4 distinct NKCL.

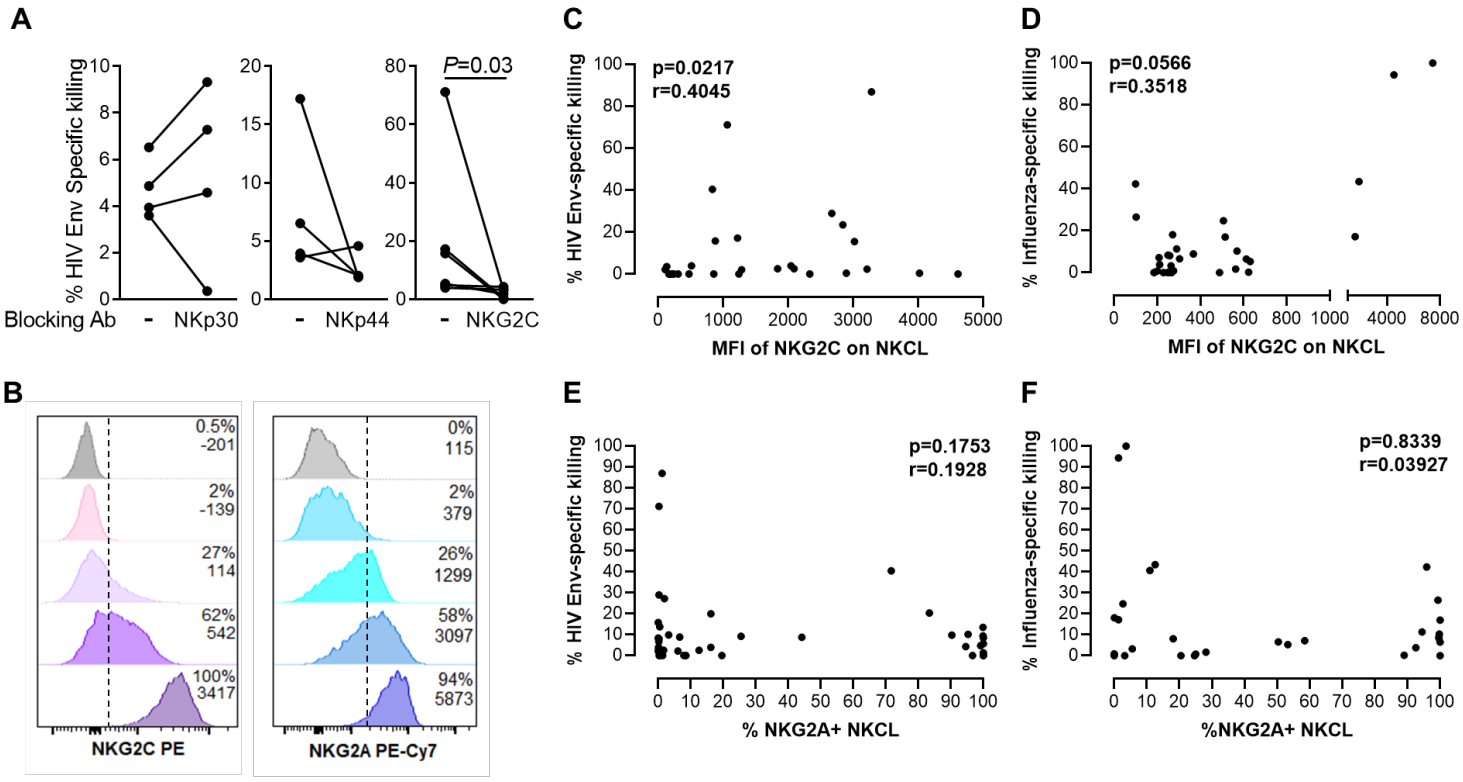

Supplementary Fig. 9. Antigen-specific NKCL responses are associated with NKG2C expression. (A) Antigen-specific killing of HIV Env-pulsed BLCL by NKCL in the presence of control or isotype control, NKp30, NKp44 or NKG2C blocking antibodies. Statistical significance was tested using Wilcoxon signed-rank tests. **(B)** Representative histograms showing NKCL with distinct NKG2C (right panel) or NKG2A expression (left panel). Frequencies of NKG2C$^+$ or NKG2A$^+$ NKCL were determined as the proportion of NKCL beyond an arbitrary cut-off line set at the right-hand side border of the NKG2C or NKG2A histogram in FMO controls (grey histograms). **(C)(D)** Spearman correlation analysis between the MFI of NKG2C on NKCL and specific killing of BLCL pulsed with HIV Env **(C)** or influenza NP, MP1, or HA **(D).** Spearman correlation analysis between frequencies of NKG2A$^+$ NKCL and specific killing of BLCL pulsed with HIV Env **(E)** or influenza NP, MP1, or HA **(F).**

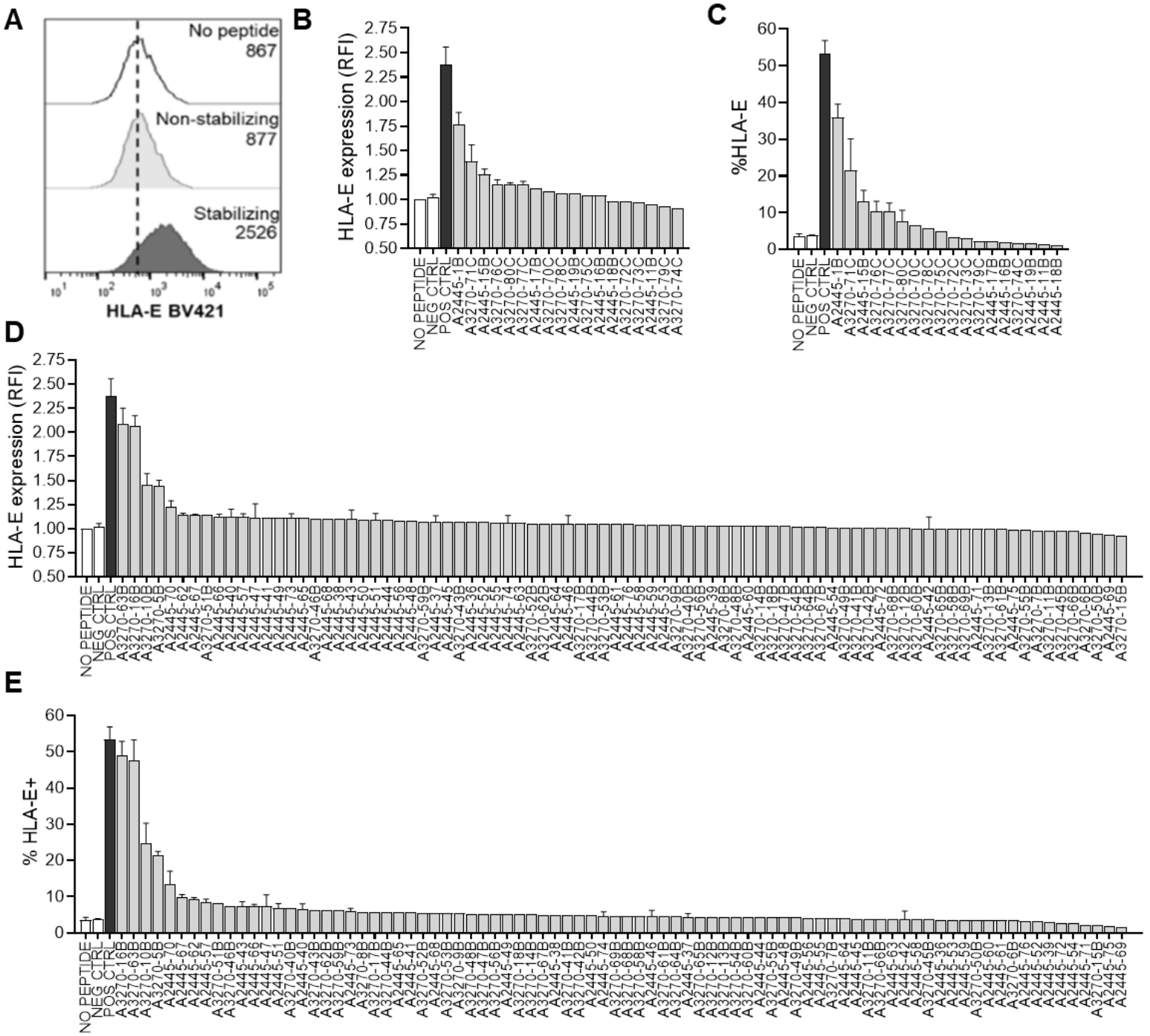
A
No peptide
867
Non-stabilizing
877
Stabilizing
2526
HLA-E BV421
B
HLA-E expression (RFI)
C
%HLA-E
D
HLA-E expression (RFI)
E
% HLA-E+

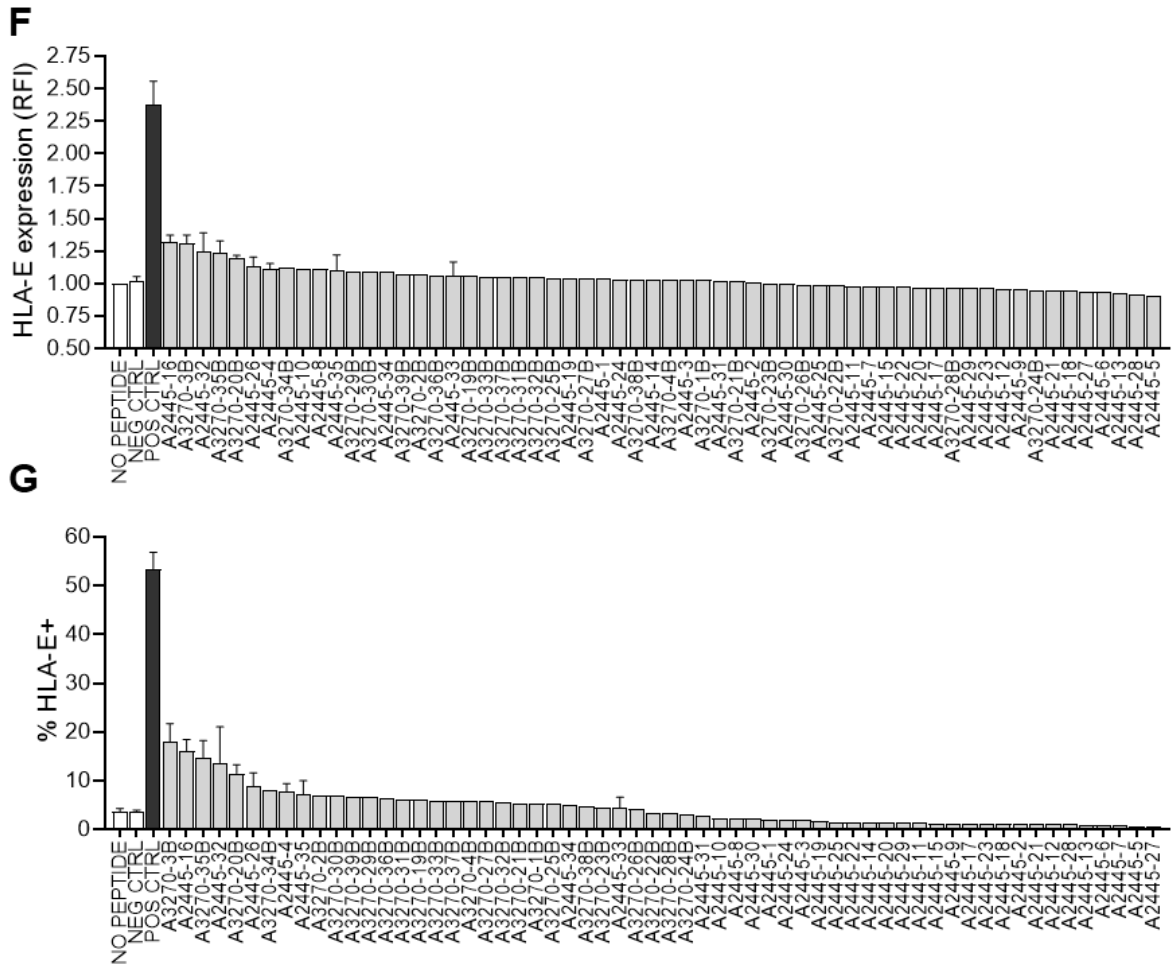

Supplementary Fig. 10. Stabilization of HLA-E*01:01 by HIV Env-, HIV Gag- and influenza NP-derived nonameric peptides. (A) Representative flow cytometry plots showing HLA-E expression on K562 stably expressing HLA-E*01:01 cells that were either left unpulsed (upper panel) or pulsed for 16 h at 26°C with 40uM of CMV-derived NLVPMVATV that do not stabilize HLA-E (middle panel), or with VMAPRTLIL, a CMV/HLA-Cw3 leader sequence-derived peptide that stabilizes HLA-E (lower panel). **(B-G)** K562 cells stably expressing HLA-E*01:01 were either left mock pulsed or pulsed for 16h with 40uM of nonameric peptides derived from A/California/04/2009(H1N1) NP (18 total) (**B-C**), HIV consensus B Env (84 total) **(D-E)** and HIV consensus B Gag (60 total) **(F-G)** with strong binding prediction scores based on the NetMHC pan 4.0 and IEDB epitope prediction tools. Controls included CMV pp65-derived NLVPMVATV that do not stabilize HLA-E (NEG CTRL), and VMAPRTLFL, a CMV/HLA-G leader sequence-derived peptide that stabilizes HLA-E (POS CTRL). HLA-E surface stabilization was assessed by flow cytometry using anti-HLA-E antibody (3D12). Dead cells were excluded. Bars represent the relative mean fluorescence intensity (RFI) + SEM of HLA-E on K562 cells as compared to HLA-E expression in the absence of peptide (No Peptide) for all tested peptides (pooled from at least 2 distinct experiments where error bars are displayed) (**B, D, F**). Mean percentages of HLA-E^{+} K562 cells + SEM are also shown for all tested peptides (**C, E, G**).

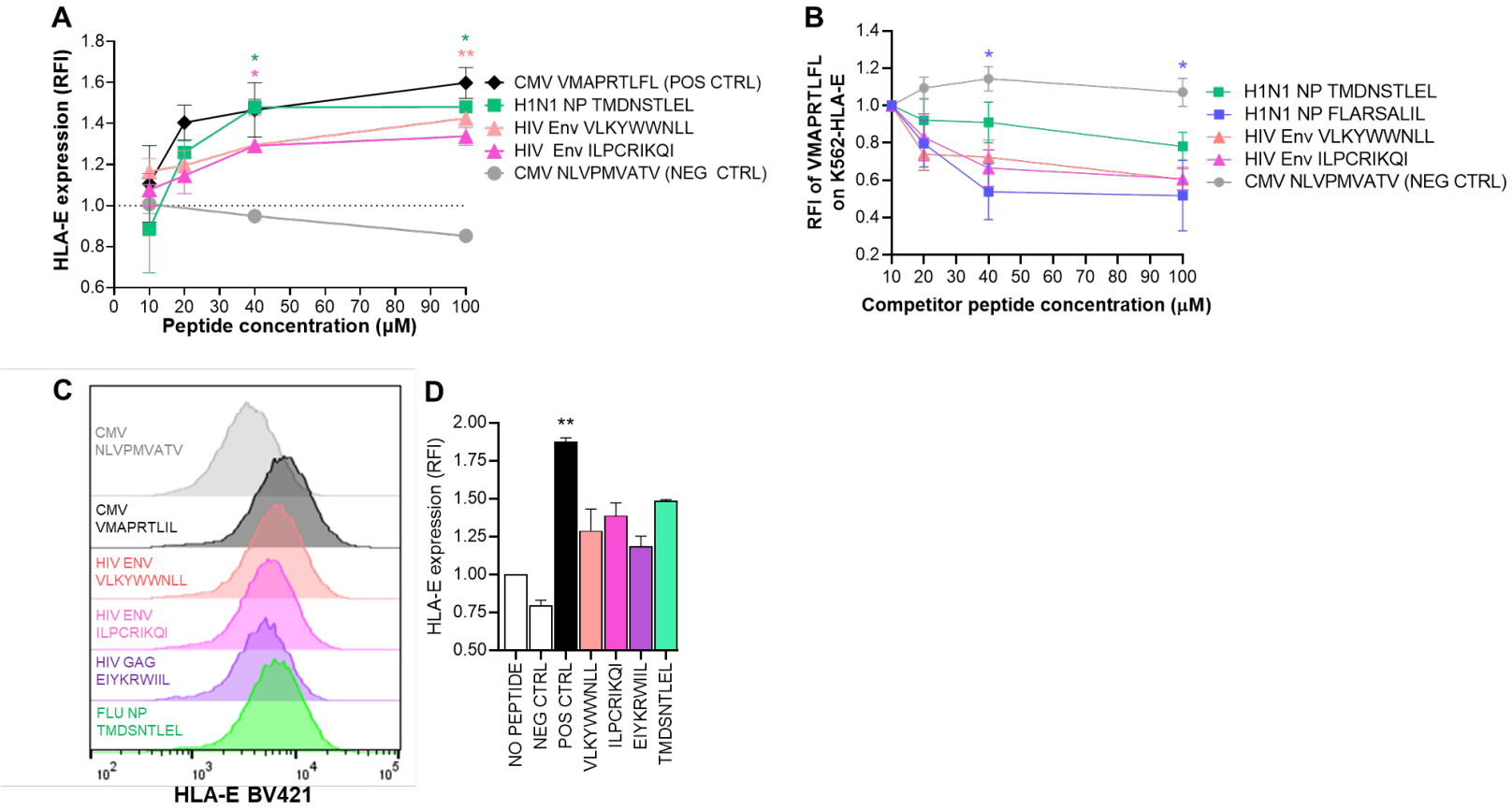

Supplementary Fig. 11. HIV Env, HIV Gag and influenza NP encode for HLA-E-stabilizing peptides. (A) Relative mean fluorescence intensity (RMFI) + SEM of HLA-E on K562 HLA-E*01:01 cells as compared to HLA-E expression in the absence of peptide after pulsing with increasing concentrations of indicated peptides (n = 2 independent experiments). Asterisks, significant differences compared to K562 HLA-E*01:01 pulsed with non-binding peptides (NEG CTRL). Statistical significance was tested using paired t tests **p<0.01, *p<0.05. **(B)** Competition assay for binding to HLA-E. K562-HLA-E*0101 cells were incubated overnight at 26°C with 10uM of FITC-conjugated VMAPRTLFL CMV peptide and increasing concentrations of the indicated unlabeled competitor peptides. Lines represent the relative mean fluorescence intensity (RFI) of HLA-E-bound FITC-labelled VMAPRTLFL peptide pooled from 3 independent experiments as compared to bound FITC-labelled VMAPRTLFL in the presence of 10uM of competitor peptide. Error bars represents the SEM. Statistical significance was tested using one-way ANOVA with Tukey's multiple comparisons test. *p<0.05. **(C-D)** HLA-E stabilization on BLCL targets after pulsing with indicated individual peptides found to stabilize HLA-E on K562 HLA-E*01:01 at 40µM for 2 hours in R10 medium. **(C)** Representative HLA-E surface detection by flow cytometry. Grey filled histogram: NLVPMVATV (NEG CTRL); back filled histogram: VMAPRTLIL (POS CTRL). **(D)** Bars represent the relative mean fluorescence intensity (RFI) + SEM of HLA-E on BLCL targets pulsed with indicated peptides pooled from 3 distinct experiments as compared to HLA-E expression in the absence of peptide (No Peptide). Statistical significance was tested using Friedman test with Dunn's multiple comparison test. Asterisks, significant differences compared to BLCL pulsed with non-binding peptides (NEG CTRL). **p<0.01.

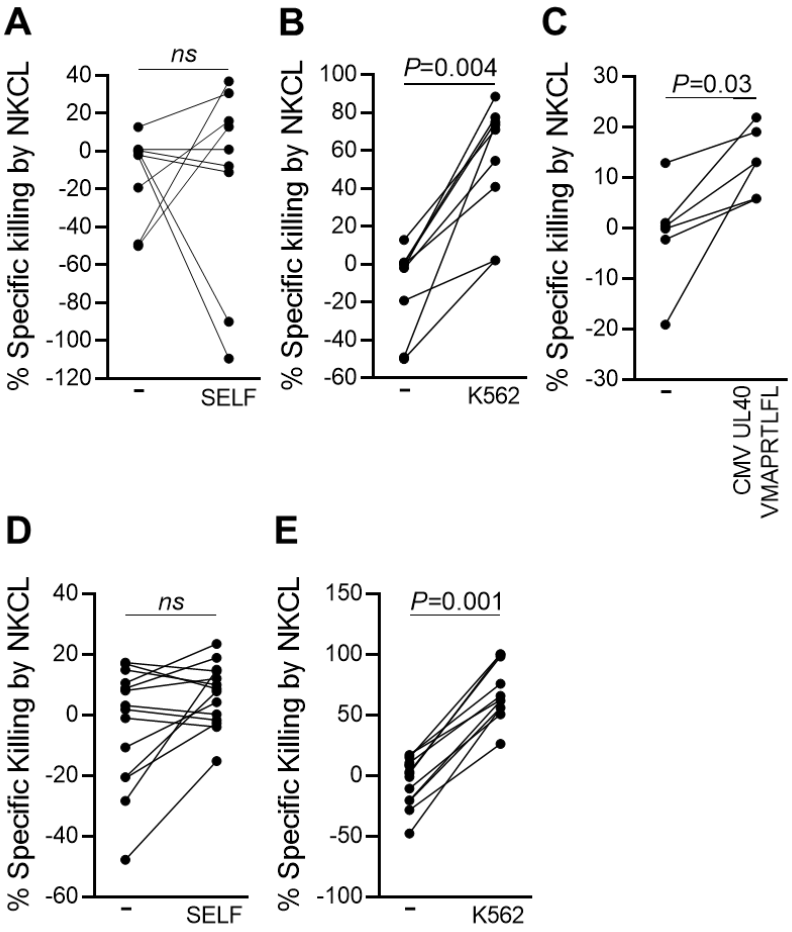

Supplementary Fig. 12. Non-specific killing by NKCL. For each NKCL generated from 5 untreated viremic PLWH (**A-C**) or from 5 healthy donors (**D-E**), paired graphs compare killing of mock pulsed autologous BLCL with percentages of non-specific lysis of self-peptide-pulsed BLCL **(A, D)**, percentages of non-specific lysis of K562 cells **(B, E)** or percentages of CMV peptide-specific killing **(C)**. CAM cytotoxicity assays were used to evaluate lysis after co-culture of NKCL with autologous BLCL pulsed with a self-peptide pool, HLA-deficient K562 cells, or a single HLA-E-binding nonameric peptides derived from CMV UL40. Statistical significance was tested using Wilcoxon signed-rank test. ns, not significant.

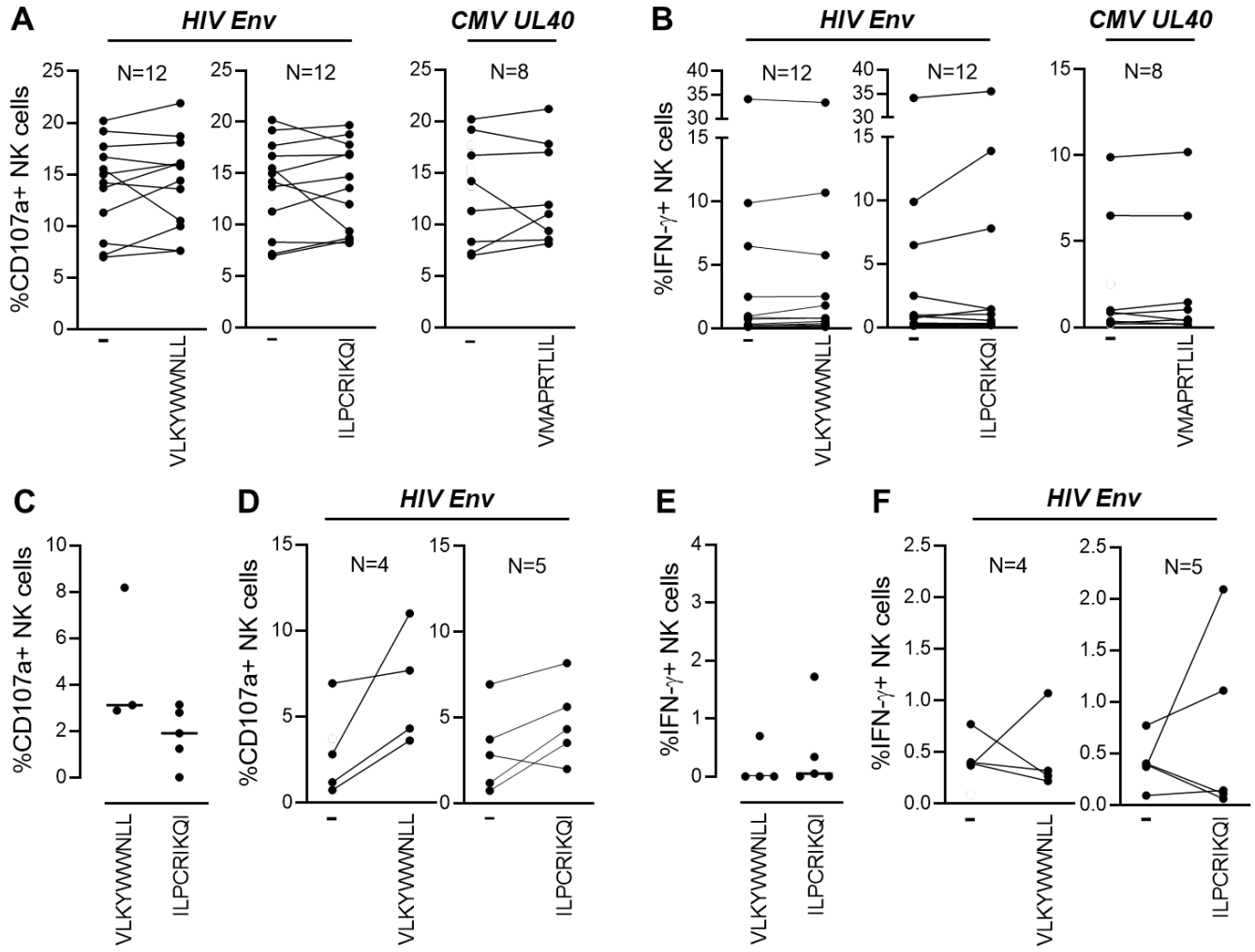

Supplementary Fig. 13. HIV Env-derived HLA-E-binding peptides elicit primary NK cell responses. Paired plots compare CD107a upregulation **(A, D)** or IFN-γ production **(B, F)** between unstimulated NK cells and NK cells stimulated with indicated single HLA-E-stabilizing peptides derived from HIV Env or CMV UL40 using ICS on unfractionated PBMC from 12 PLWH (**A-B**) or enriched NK cells from 5 PLWH (**C-F**). **C, E,** Dot plots compare proportions of actively degranulating, cytotoxic NK cells, as judged by expression of CD107a **(C)** or IFN-γ producing NK cells **(E)** from 5 PLWH in response to indicated HLA-E-stabilizing single peptides after subtracting proportions of $CD107a^+$ and $IFN\text{-}\gamma^+$ unstimulated NK cells, respectively. Bars represent the median. Statistical significance was tested using Wilcoxon signed-rank test and p-values found not statistically significant (P>0.05).

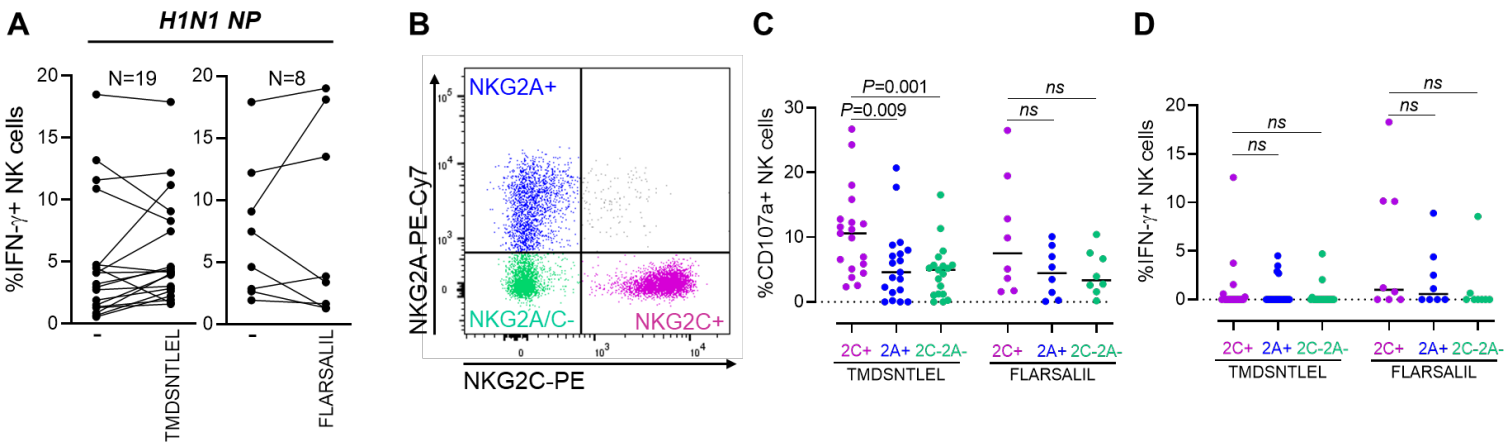

Supplementary Fig. 14. Influenza NP-derived HLA-E-binding peptides elicit primary NKG2C+ NK cell responses. (A) Paired plots compare IFN-y production between unstimulated NK cells and NK cells stimulated with indicated single HLA-E-stabilizing peptides derived from influenza NP using ICS on enriched NK cells from 19 healthy donors. **(B)** Representative staining for NKG2A and NKG2C at the surface of $CD56^{+}CD16^{+/-}$ NK cells from an HIV-negative healthy donor by flow cytometry. **C, D,** Dot plots compare proportions of actively degranulating, cytotoxic $NKG2C^{+}$ (purple dots), $NKG2A^{+}$ (blue dots), and $NKG2C^{-}NKG2A^{-}$ (green dots) NK cells, as judged by expression of CD107a **(C)** or $NKG2C^{+}$ (purple dots), $NKG2A^{+}$ (blue dots) and $NKG2C^{-}NKG2A^{-}$ (green dots) IFN-γ producing NK cells **(D)** from 19 healthy donors in response to indicated HLA-E-stabilizing single peptides after subtracting proportions of $CD107a^{+}$ and IFN-γ^{+} unstimulated NK cells, respectively. Bars represent the median. Statistical significance was tested using Wilcoxon signed-rank test **(A)** or Friedman test with Dunn's multiple comparison test (**C-D**). ns, not significant.

Supplementary Table 1. Characteristics of PLWH and healthy donors				
Clinical Data	**Viremic (n=27)**	**cART treated (n=21)**	**elite controllers (n=4)**	**HIV-negative (n=66)**
Median HIV viral load [IQR] (RNA cop/mL)	14,100 [28,790]	<50	<50	NA
Median CD4 cell count [IQR] (cells/mm3)	599 [286]	624 [355]		NA
N with available clinical data	26	3	0	NA

PLWH, People living with HIV; cART, combination antiretroviral therapy; IQR, interquartile range; NA, not applicable

Supplementary Table 2. 28-color panel for NKCL phenotyping			
Target	**Fluorochrome**	**Clone**	**Manufacturer**
LIVE cells	Blue Live/Dead		Invitrogen
CD19	PE-CY5.5	J3-119	BECKMAN COULTER
CD14	BUV615	M5E2	BD Pharmingen
CD3	BUV496	UCHT1	BD Pharmingen
CD4	BB700	L200	BD Pharmingen
CD56	BUV737	NCAM16.2	BD Pharmingen
CD16	BUV563	3G8	BD Pharmingen
NKP46	BV711	9E2/NKp46	BD Pharmingen
NKG2D	BB790	1D11	BD Pharmingen
NKG2C	Biotin + SA BUV395	REA205	MILTENYI
NKG2A	PE-CY7	Z199	BECKMAN COULTER
KIR3DL1/S1	VioBlue	REA168	MILTENYI
KIR2DL1/S1/S3/S5	FITC	HP-MA4	BIOLEGEND
KIR2DS4	APC-Vio770	REA284	MILTENYI
CD85J	PE	GHI/75	BD Pharmingen
$\alpha 4\beta 7$	APC		NHP Reagent Resource
CXCR6	BV786	13B 1E5	BD Pharmingen
CCR5	PE-CY5	2D7/CCR5	BD Pharmingen
CCR7	APC-R700	3D12	BD Pharmingen
2B4	BV650	2-69	BD Pharmingen
CD2	BV510	2H7	BD Pharmingen
CD8	BV570	RPA-T8	BIOLEGEND
CD57	BB630	NK-1	BD Pharmingen
KLRG1	PE-Dazzle594	2F1/KLRG1	BIOLEGEND
PD1	BV605	EH12.1	BD Pharmingen
TIM-3	BV750	7D3	BD Pharmingen
HLA-DR	BUV661	G46-6	BD Pharmingen
IL-7R	BUV805	HIL-7R-M21	BD Pharmingen

Supplementary Table 3. HIV- and influenza-derived nonamers tested for binding to HLA-E*01:01

HIV Gag

ID	Sequence	Position
A2445-1	VWASRELER	35
A2445-2	SRELERFAV	38
A2445-3	ERFAVNPGL	42
A2445-4	ILGQLQPSL	60
A2445-5	QVSQNYPIV	127
A2445-6	QNYPIVQNL	130
A2445-7	VHQAISPRT	143
A2445-8	VVEEKAFSP	158
A2445-9	FSPEVIPMF	164
A2445-10	PEVIPMFSA	166
A2445-11	QMLKETINE	199
A2445-12	HAGPIAPGQ	219
A2445-13	WMTNNPPIP	249
A2445-14	TNNPPIPVG	251
A2445-15	IVRMYSPTS	273
A2445-16	RMYSPTSIL	275
A2445-17	YSPTSILDI	277
A2445-18	RQGPKEPFR	286
A2445-19	QGPKEPFRD	287
A2445-20	RDYVDRFYK	294
A2445-21	VKNWMTETL	313
A2445-22	ILKALGPAA	333
A2445-23	LGPAATLEE	337
A2445-24	RVLAEAMSQ	361
A2445-25	VTNSATIMM	370
A2445-26	IMMQRGNFR	376
A2445-27	MMQRGNFRN	377
A2445-28	RKTVKCFNC	387
A2445-29	AKNCRAPRK	402
A2445-30	TERQANFLG	427
A2445-31	KGRPGNFLQ	442
A2445-32	RPEPTAPPE	452
A2445-33	APPEESFRF	457
A2445-34	IDKELYPLA	479
A2445-35	SLFGNDPSS	491
A3270-1B	YVDRFYKTL	296
A3270-2B	SLYNTVATL	77
A3270-3B	KALGPAATL	335
A3270-4B	ATPQDLNTM	179
A3270-19B	SLQTGSEEL	67
A3270-20B	RFAVNPGLL	43

HIV Env

ID	Sequence	Position
A2445-36	LWRWGTMLL	13
A2445-37	TMLLGMLMI	18
A2445-38	VWKEATTTL	43
A2445-39	EATTTLFCA	46
A2445-40	ATHACVPTD	69
A2445-41	ENVTENFNM	86
A2445-42	QMHEDIISL	102
A2445-43	IISLWDQSL	107
A2445-44	VQKEYALFY	168
A2445-45	QKEYALFYK	169
A2445-46	VITQACPKV	200
A2445-47	ACPKVSFEP	204
A2445-48	VSFEPIPIH	208
A2445-49	CAPAGFAIL	218
A2445-50	KCNDKKFNG	227
A2445-51	IRPVVSTQL	251
A2445-52	VIRSENFTD	271
A2445-53	IGPGRAFYT	309
A2445-54	GNKTIVFNQ	353
A2445-55	CNTTQLFNS	383
A2445-56	TKDKNTITL	402
A2445-57	TLPCRIKQI	409
A2445-58	NNDTEIFRP	456
A2445-59	VAPTKAKRR	490
A2445-60	VGIGAMFLG	507
A2445-61	TMGAASMTL	523
A2445-62	TLTVQARQL	530
A2445-63	TVQARQLLS	532
A2445-64	AIEAQQHLL	552
A2445-65	IKQLQARVL	567
A2445-66	QLQARVLAV	569
A2445-67	RVLAVERYL	573
A2445-68	ICTTTVPWN	597
A2445-69	LWYIKIFIM	673
A2445-70	IMIVGGLIG	680
A2445-71	IGLRIVFAV	687
A2445-72	VRQGYSPLS	702
A2445-73	GYSPLSFQT	705
A2445-74	QTRLPAPRG	712
A2445-75	LPAPRGPDR	715
A2445-76	IVTRIVELL	771

A/California/7/2009(H1N1) NP

ID	Sequence	Position
A2445-1B	TMDSNTLEL	373
A2445-11B	LRGSVAHKS	266
A2445-15B	FLARSALIL	258
A2445-16B	LMQGSTLPR	166
A2445-17B	VIPRGKLST	352
A2445-18B	GMDPRMCSL	158
A2445-19B	MMESAKPED	447
A3270-70C	ATYQRTRAL	146
A3270-71C	ATNPIVPSF	471
A3270-72C	RLIQNSITI	55
A3270-73C	RMIGGIGRF	31
A3270-74C	MSNEGSYFF	481
A3270-75C	ASNENVETM	366
A3270-76C	ATAGLTHIM	129
A3270-77C	KLSTRGVQI	357
A3270-78C	VGIDPFKLL	299
A3270-79C	WMACHSAAF	343
A3270-80C	VAYERMCNI	230

A3270-21B	HQAISPRTL	144
A3270-22B	VLAEAMSQV	362
A3270-23B	KQEPIDKEL	475
A3270-24B	AMQMLKETI	197
A3270-25B	AGPIAPGQM	220
A3270-26B	RQANFLGKI	429
A3270-27B	HIVWASREL	33
A3270-28B	SQVTNSATI	368
A3270-29B	MTNNPPIPV	250
A3270-30B	AFSPEVIPM	163
A3270-31B	EVIPMFSAL	167
A3270-32B	RTLNAWVKV	150
A3270-33B	YPLASLRSL	484
A3270-34B	ASQEVKNWM	309
A3270-35B	EIYKRWIIL	260
A3270-36B	RAEQASQEV	305
A3270-37B	ASVLSGGEL	5
A3270-38B	VRMYSPTSI	274
A3270-39B	ISPRTLNAW	147

A3270-5B	LLQYWSQEL	795
A3270-6B	CSSNITGLL	440
A3270-7B	IVQQQNNLL	544
A3270-8B	KLTPLCVTL	120
A3270-9B	KVQKEYALF	167
A3270-10B	RLVDGFLAL	743
A3270-11B	RVRQGYSPL	703
A3270-12B	SSNITGLLL	441
A3270-13B	CTDLKNNLL	130
A3270-14B	FSDNANTII	288
A3270-15B	HMGPGRALF	319
A3270-16B	ILPCRIKQI	423
A3270-17B	LLQYWSQEL	793
A3270-18B	STPLADGFL	756
A3270-40B	ASLWNWFDI	663
A3270-41B	AVGIGAMFL	508
A3270-42B	FFYCNTTQL	380
A3270-43B	FLGAAGSTM	518
A3270-44B	FSYHRLRDL	762
A3270-45B	FTNNAKTII	277
A3270-46B	HLWRWGTML	12
A3270-47B	IGAMFLGFL	511
A3270-48B	KVSFEPIPI	207
A3270-49B	LGRRGWEVL	781
A3270-50B	LISCNTSVI	193
A3270-51B	LLGRRGWEV	780
A3270-52B	LTVQARQLL	533
A3270-53B	LVDGFLALI	744
A3270-54B	RAFYTTGEI	313
A3270-55B	RAIEAQQHL	553
A3270-56B	RQGLERALL	844
A3270-58B	RYLKDQQLL	581
A3270-59B	SLDEIWDNM	614
A3270-60B	STVQCTHGI	243
A3270-61B	SYHRLRDLL	763
A3270-62B	VLENVTENF	83
A3270-63B	VLKYWWNLL	788
A3270-64B	VSLLNATAI	808
A3270-65B	VTLNCTDLM	126
A3270-66B	VVQRACRAI	828
A3270-67B	YAPPIRGQI	430
A3270-68B	YHRLRDLLL	764
A3270-69B	YTSLIYTLI	634